Available online at www.sciencedirect.com

ScienceDirect

IFAC PapersOnLine 50-1 (2017) 4324–4329

Using iterative LQR to control two quadrotors transporting a cable-suspended load

Yaser Alothman * **Minhuan Guo** ** **Dongbing Gu** ***

* *School of Computer Science and Electronic Engineering, University of Essex, Wivenhoe Park, Colchester, UK.(e-mail: ynialo@essex.ac.uk),University of Technology, Baghdad, Iraq.*
** *Nanjing University of Science and Technology. (e-mail: 312012201@njust.edu.cn)*
*** *School of Computer Science and Electronic Engineering, University of Essex, Wivenhoe Park, Colchester, UK. (e-mail: dgu@essex.ac.uk)*

Abstract: This paper is focused on the tracking control problem of two quadrotors carrying one cable-suspended payload. The paper main contributions include a dynamic model constructed by Euler-Lagrange equations for this system, an iterative linear quadratic regulator (iLQR) optimal controller, which is able to track the desired trajectory for the payload position and attitude and a simulation for tracking a spiral trajectory. The nonlinear dynamic model is linearised by considering the angles of connected links from the payload to each quadrotor as the equilibrium point. The iLQR control algorithm is developed for the full system consisting of two quadrotors connected with a point mass load in order to improve the tracking performance and avoid the slung load swing. The simulation results demonstrate that the iLQR approach is able to improve the tracking performance compared with an LQR controller.

Keywords: iLQR Controller, payload carrying, quadrotor tracking control, Euler-Lagrange method.

1. INTRODUCTION

The research area of quadrotors transporting cable-suspended payload is growing worthily with a wide range of various applications. In recent decades, the maturation has been seen for civil and military applications in different research areas such as emergency rescue, reconnaissance, fire-fighting, freight transportation mission, etc. The prominent key task to be considered here is transporting a slung load via two quadrotors connected by cables. However, because of the system uncertainties, the high non-linearity of dynamic model, and the swing of heavy suspended load, it remains a challenging task for controller design. Due to significant tension forces applied to small light vehicles, the load impact on the underlying system dynamics should not be neglected. The changes in operating point induced by the slung load also cause the problem for linearised systems Trachte et al. (2015). The control objectives include not only the stabilisation of quadrotors, but also achieving minimum fluctuation of the suspended payload while tracking a desired trajectory.

Different studies have been introduced of transporting cable suspended payload using a nonlinear control system to achieve the stability with one quadrotor. In Klausen et al. (2015) Kane's method is presented for the system considering the load as a pendulum. A nonlinear controller is derived based on the backstepping technique and the simulation results are provided. A combination of modern control approaches is implemented for single quadrotor with a slung load in Lee et al. (2015) where a neural network is designed to control the attitude and the entire system is developed based on the Udwadia-Kalaba equation. A geometric control is constructed to improve the performance of controlling a cable suspended payload with multiple quadrotors following a desired trajectory in Wu and Sreenath (2014), where a coordinate-free dynamical model is developed based on the equations of motions then a geometric feedback control is designed. The authors in Lee et al. (2013) and Lee (2014) consider the tracking controller based on coordinate-free fashion development. Similarly in Sreenath and Kumar (2013) a complete dynamic model is developed for both point mass and rigid body using differential flatness technique for payload and quadrotors to follow a desired trajectory. Most non-linear controllers are able to stabilise the control system but the dynamic performance can not be optimised.

The authors in Trachte et al. (2015) propose a Nonlinear Model Predictive Control (NMPC) to manage the nonlinear dynamics with the constraints to track waypoints precisely and restrain payload large angles. A Linear Quadratic Regulator (LQR) controller is derived in order to compare the performance with NMPC in simulation and the improvement on the cost function during aggressive maneuveres is demonstrated. Such research is restrictive to one quadrotor carrying one suspended payload. A LQR controller is proposed by researchers Alothman et al. (2015) for one quadrotor to overcome the challenges whilst transporting the load. A combination control of

Peer review under responsibility of International Federation of Automatic Control.
10.1016/j.ifacol.2017.08.861

linear quadratic regulator (LQR) and sliding mode control (SMC) is used for leader and follower formation maintenance Ghamry and Zhang (2015). The inner and outer loops for position and attitude are improved during trajectory tracking.

LQR controllers are able to optimise the control performance. However, the changes in operating point when non-linearity is high and the change induced by the slung load for linearised systems should not be ignored. The iterative LQR (iLQR) is able to reduce the changes in operation point via multiple iterations. The researchers propose a sequential linear quadratic (SLQ) and iterative linear quadratic Gussian (iLQG) controllers in de Crousaz et al. (2015) and de Crousaz et al. (2014) to achieve the stability with aggressive manoeuvres for one quadrotor carrying one suspended payload.

In this paper, an iLQR optimal controller with quadratic approximation is developed via dynamic programming approach for the transportation task where a load is suspended by cables with two quadrotor. The design of the iLQR controller is based on LQR method. Th control objective is for the point mass payload to follow a desired trajectory in position and attitude. The test of system performance is conducted in an aggressive spiral trajectory to demonstrate the complexities of the nonlinear system by the comparison with a LQR controller.

In the following, Section 2 presents the precise mathematical model of a cable suspended payload by two quadrotors. Section 3 illustrates the derivation of the iLQR control approach fundamentals. Section 4 shows the simulation results in different trajectories. The conclusion and suggestions for future work are introduced in Section 5.

2. MODEL DESCRIPTION

2.1 System and Notations

The full system is presented Fig. 1 including the inertial frame, intermediate frame, body-fixed frame, vertical and horizontal forces generated by each propeller and swing angles of the rope with respect to the intermediate frame.

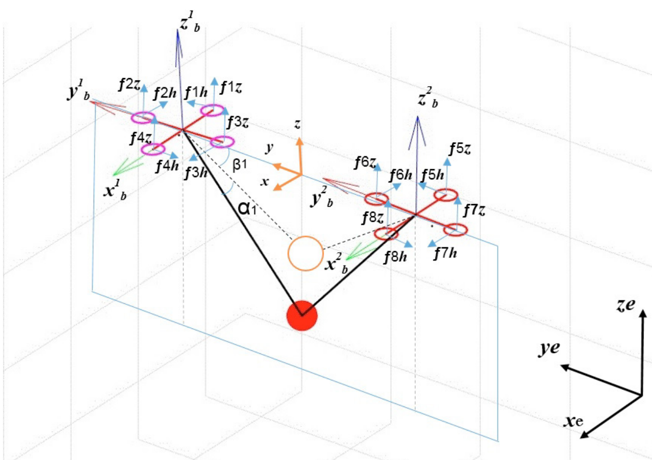

Fig. 1. Two quadrotors carrying paload plant

In order to simplify the problem, some reasonable hypotheses are given as follows:

(1) The quadrotor is considered as a symmetrical rigid body.
(2) The payload is considered as a point mass and is attached at the centre of the quadrotor.
(3) The cable tension is always non-zero.
(4) The air drag of the propellers is negligible.

Partial symbols and acronyms used in this paper are listed in table 1.

Table 1. Symbols and Definitions

Symbol	Description
$\boldsymbol{S_e : x_e y_e z_e}$	Inertial frame
$\boldsymbol{S^k : xyz}$	Intermediate frame: translate $\boldsymbol{S_e}$ to the center of the kth quadrotors $k = 1, 2$
$\boldsymbol{S_b^k : x_b^k y_b^k z_b^k}$	Body-fixed frame for quadrotor,
$\boldsymbol{E}_i \in \mathbb{R}^3, i = 1, 2, 3$	Unit orthogonal vectors of $\boldsymbol{S_e}$
$\boldsymbol{e}_i^k \in \mathbb{R}^3, i = 1, 2, 3$	Unit orthogonal vectors of $\boldsymbol{S_b^k}$
$\boldsymbol{\eta}^k = [\phi, \theta, \psi]^T \in \mathbb{R}^3$	Euler angles of quadrotor defined in $Z - Y - X$
$\boldsymbol{T}_{e2b}^k \in \mathbb{R}^{3\times3}$	Transformation matrix from $\boldsymbol{S_e}$ to $\boldsymbol{S_b^k}$
$\boldsymbol{\Omega}^k \in \mathbb{R}^3$	Angular velocity of quadrotor in $\boldsymbol{S_b^k}$
m_Q^k	Mass of the quadrotor
m_P	Mass of the payload
$\boldsymbol{I}_Q^k \in \mathbb{R}^3$	Inertial matrix of the quadrotor with respect to $\boldsymbol{S_b^k}$
$\boldsymbol{\xi}_Q^k \in \mathbb{R}^3$	Position of the center of quadrotor in $\boldsymbol{S_e}$
$\boldsymbol{\xi}_P \in \mathbb{R}^3$	Position of the payload in $\boldsymbol{S_e}$
L_r^k	Length of the rope
L_Q^k	Length of the quadrotor arm
$\alpha_k, \beta_k \in \mathbb{R}$	Angles of the rope with respect to $\boldsymbol{S^k}$
$\boldsymbol{\rho}^k \in \mathbb{R}^3$	Unit vector from the payload to the attached point
$\boldsymbol{f}_{iz}^k, \boldsymbol{f}_{ih}^k \in \mathbb{R}^3$	Vertial and horizontal forces generated by ith propeller, $i = 1, 2, 3, 4$
$k_F, k_M \in \mathbb{R}$	Propeller aerodynamic parameters

The following relationships are available.

$$
\begin{aligned}
\boldsymbol{\rho}^k &= \left[-sin(\beta^k), -cos(\alpha^k)cos(\beta^k), sin(\alpha^k)cos(\beta^k)\right]^T \\
\boldsymbol{\xi}_P &= x_P\boldsymbol{E_1} + y_P\boldsymbol{E_2} + z_P\boldsymbol{E_3} \\
\boldsymbol{\xi}_Q^k &= \boldsymbol{\xi}_P + L_r^k\boldsymbol{\rho}^k \\
\boldsymbol{\Omega}^k &= \begin{bmatrix} 1 & 0 & -sin(\theta^k) \\ 0 & cos(\phi^k) & sin(\phi^k)cos(\theta^k) \\ 0 & -sin(\phi^k) & cos(\phi^k)cos(\theta^k) \end{bmatrix} \begin{bmatrix} \dot{\phi}^k \\ \dot{\theta}^k \\ \dot{\psi}^k \end{bmatrix}
\end{aligned} \tag{1}
$$

2.2 Euler-Lagrange Modeling

The quadrotor-payload system has 13 degrees of freedom. Choosing $\boldsymbol{q} = \left[x_P, y_P, z_P, \alpha^1, \beta^1, \phi^1, \theta^1, \psi^1, \alpha^2, \beta^2, \phi^2, \theta^2, \psi^2\right]^T$ as the generalized coordinates will not only be convenient while controlling the trajectory of the payload but also be helpful for extending to multi-vehicle situations. As a result, the Lagrangian $\mathfrak{L}$ is composed by subtraction of the kinetic and potential energies denoted by $\mathfrak{T}$ and $\mathfrak{U}$ as clarified in equations

$$\begin{aligned}
&\mathfrak{T} = \frac{1}{2}m_P{\boldsymbol{\xi}_P}^T \cdot \boldsymbol{\xi}_P + \frac{1}{2}m_Q^1{\boldsymbol{\xi}_Q^1}^T \cdot \boldsymbol{\xi}_Q^1 + \frac{1}{2}(\boldsymbol{\Omega}^1)^T \boldsymbol{I}_Q^1 \boldsymbol{\Omega}^1 \\
&\quad \frac{1}{2}m_Q^2{\boldsymbol{\xi}_Q^2}^T \cdot \boldsymbol{\xi}_Q^2 + \frac{1}{2}(\boldsymbol{\Omega}^2)^T \boldsymbol{I}_Q^2 \boldsymbol{\Omega}^2 \\
&\mathfrak{U} = m_P g \boldsymbol{\xi}_P \cdot \boldsymbol{E}_3 + m_Q^1 g \boldsymbol{\xi}_Q^1 \cdot \boldsymbol{E}_3 + m_Q^2 g \boldsymbol{\xi}_Q^2 \cdot \boldsymbol{E}_3 \\
&\mathfrak{L} = \mathfrak{T} - \mathfrak{U}
\end{aligned} \tag{2}$$

Then the Euler-Lagrange equation is

$$\frac{d}{\mathrm{dt}}\left(\frac{\partial L}{\partial \dot{\boldsymbol{q}}}\right) - \frac{\partial L}{\partial \boldsymbol{q}} = \boldsymbol{Q} \tag{3}$$

The generalized force $\boldsymbol{Q}$ defined here is based on the choice of the generalized coordinates $\boldsymbol{q}$ and the external conservative forces $\sum \boldsymbol{F}_i$. For each quadrotor, the force $\boldsymbol{F}_i$ consists of two complements $\boldsymbol{f}_{iz}$ and $\boldsymbol{f}_{ih}$ (equation (4)) which are related with the angular speed ω_i of ith propeller.

$$\begin{aligned}
\boldsymbol{F}_i^k &= \boldsymbol{f}_{iz}^k + \boldsymbol{f}_{ih}^k, i = 1,2,3,4 \\
\boldsymbol{f}_{iz}^k &= k_F \omega_i^2 \boldsymbol{e}_3^k, i = 1,2,3,4 \\
\boldsymbol{f}_{1h}^k &= k_M \omega_1^2 \boldsymbol{e}_2^k \\
\boldsymbol{f}_{2h}^k &= k_M \omega_2^2 \boldsymbol{e}_1^k \\
\boldsymbol{f}_{3h}^k &= -k_M \omega_3^2 \boldsymbol{e}_2^k \\
\boldsymbol{f}_{4h}^k &= -k_M \omega_4^2 \boldsymbol{e}_1^k
\end{aligned} \tag{4}$$

where $\boldsymbol{e}_i^k = \boldsymbol{T}_{e2b}^k \boldsymbol{E}_i$, $i = 1,2,3$.

As seen in Fig. 1, the point where the force $\boldsymbol{F}_i^k$ is applied on is the centre of each propeller and the corresponding position vector is noted as $\boldsymbol{\xi}_i^k$ seen in equation (5).

$$\begin{aligned}
\boldsymbol{\xi}_1^k &= \boldsymbol{\xi}_Q^k + L_Q \boldsymbol{e}_1^k \\
\boldsymbol{\xi}_2^k &= \boldsymbol{\xi}_Q^k + L_Q \boldsymbol{e}_2^k \\
\boldsymbol{\xi}_3^k &= \boldsymbol{\xi}_Q^k - L_Q \boldsymbol{e}_1^k \\
\boldsymbol{\xi}_4^k &= \boldsymbol{\xi}_Q^k - L_Q \boldsymbol{e}_2^k
\end{aligned} \tag{5}$$

According to the principle of virtual work, the generalized forces are given by equation (6).

$$Q_i = \sum_{j=1}^{4} \sum_{k=1}^{2} \frac{\partial(\boldsymbol{F}_j^k \cdot \boldsymbol{\xi}_j^k)}{\partial q_i}, i = 1,2,..,13 \tag{6}$$

Taking the generalized forces and equation (2) into equation (3), the Euler-Lagrange equation can be rewritten in

$$\boldsymbol{M}\ddot{\boldsymbol{q}} = f(\boldsymbol{q}, \dot{\boldsymbol{q}}) \tag{7}$$

Considering the balance situation as the equilibrium point $(\boldsymbol{x}_0, \boldsymbol{u}_0)$, the linearised model is obtained in equation (8).

$$\ddot{\boldsymbol{q}} = \boldsymbol{M}^{-1} \left.\frac{\partial f}{\partial \boldsymbol{x}}\right|_{\boldsymbol{x}_0} \Delta \boldsymbol{x} + \boldsymbol{M}^{-1} \left.\frac{\partial f}{\partial \boldsymbol{u}}\right|_{\boldsymbol{u}_0} \Delta \boldsymbol{u} \tag{8}$$

Furthermore, equation (8) can be stated in the following standard state-space form.

$$\begin{aligned}
\dot{\boldsymbol{x}} &= \boldsymbol{A}\boldsymbol{x} + \boldsymbol{B}\boldsymbol{u} \\
\boldsymbol{y} &= \boldsymbol{C}\boldsymbol{x}
\end{aligned} \tag{9}$$

where $\boldsymbol{A} \in \mathbb{R}^{26\times 26}$, $\boldsymbol{B} \in \mathbb{R}^{26\times 8}$ and $\boldsymbol{C} = \boldsymbol{I}^{26\times 26}$.
$\boldsymbol{x} = [x_P, \dot{x}_P, y_P, \dot{y}_P, z_P, \dot{z}_P, \alpha^1, \dot{\alpha}^1, \beta^1, \dot{\beta}^1, \phi^1, \dot{\phi}^1, \theta^1, \dot{\theta}^1, \psi^1, \dot{\psi}^1, \alpha^2, \dot{\alpha}^2, \beta^2, \dot{\beta}^2, \phi^2, \dot{\phi}^2, \theta^2, \dot{\theta}^2, \psi^2, \dot{\psi}^2]^T \in \mathbb{R}^{26}$,
$\boldsymbol{u} = [\omega_1, \omega_2, \omega_3, \omega_4, \omega_5, \omega_6, \omega_7, \omega_8]^T \in \mathbb{R}^8, \boldsymbol{y} \in \mathbb{R}^{26}$

3. ITERATIVE LQR CONTROLLER

The main aim of this paper is to develop and implement an iterative LQR optimal controller. This optimal control method provides an iterative technique such that the non-linear dynamic model is subjected to linearisation in each iteration and iteratively the cost function around the nominal requirement result is obtained. The discrete-time non-linear dynamical model is

$$\boldsymbol{x}_{\mathbf{t}+1} = f(\boldsymbol{x}_{\mathbf{t}}, \boldsymbol{u}_{\mathbf{t}}). \tag{10}$$

The quadratic form cost function is

$$\begin{aligned}
J =& 1/2(\boldsymbol{x}_N - \boldsymbol{x}^*)^T Q_f (\boldsymbol{x}_N - \boldsymbol{x}^*) \\
&+ 1/2 \sum_{\mathbf{t}=0}^{N-1} (\boldsymbol{x}_{\mathbf{t}}^T Q \boldsymbol{x}_{\mathbf{t}} + \boldsymbol{u}_t^T R \boldsymbol{u}_{\mathbf{t}}).
\end{aligned} \tag{11}$$

The initial requirements of the iLQR method are presented by a nominal control sequence and a corresponding trajectory represented by $\boldsymbol{x}_{\mathbf{t}}$ and $\boldsymbol{u}_{\mathbf{t}}$, respectively. The nominal state is acquired from applying $\boldsymbol{u}_{\mathbf{t}}$ to the open loop dynamical model iteratively. Through each iteration, the improved sequence $\boldsymbol{u}_{\mathbf{t}}$ is obtained by linearising the nonlinear dynamics of the system around nominal control $\boldsymbol{u}_{\mathbf{t}}$ and state $\boldsymbol{x}_{\mathbf{t}}$. Then the convergence is achieved by proceeding refined iteration due to the control deviation $\delta\boldsymbol{u}_{\mathbf{t}}$ and state $\delta\boldsymbol{x}_{\mathbf{t}}$ from the desired control and state relying on solved the modified LQR problem Li and Todorov (2004),Zhang et al. (2012). where the final and target states are denoted by x_N and $\boldsymbol{x}^*$ with N steps respectively.The system linearisation is

$$\delta\boldsymbol{x}_{\mathbf{t}+1} = \boldsymbol{A}_{\mathbf{t}}\delta\boldsymbol{x}_{\mathbf{t}} + \boldsymbol{B}_{\mathbf{t}}\delta\boldsymbol{u}_{\mathbf{t}}. \tag{12}$$

The first step is started with the Hamiltonian function to proceed with the optimal control $\delta\boldsymbol{u}_{\mathbf{t}}$ represented as:

$$\begin{aligned}
H_{\mathbf{t}} =\ & (\boldsymbol{x}_{\mathbf{t}} + \delta\boldsymbol{x}_{\mathbf{t}})^T Q (\boldsymbol{x}_{\mathbf{t}} + \delta\boldsymbol{x}_{\mathbf{t}}) \\
&+ (\boldsymbol{u}_{\mathbf{t}} + \delta\boldsymbol{u}_{\mathbf{t}})^T R (\boldsymbol{u}_{\mathbf{t}} + \delta\boldsymbol{u}_{\mathbf{t}}) \\
&+ \lambda_{\mathbf{t}+1}^T (A_{\mathbf{t}}\delta\boldsymbol{x}_{\mathbf{t}} + B_{\mathbf{t}}\delta u_{\mathbf{t}}).
\end{aligned}$$

Where λ_{t+1}^T is denoted by lagrange multiplier. The required derivatives of the Hamiltonian function are:

$$\partial H_{\mathbf{t}}/\partial(\delta\boldsymbol{x}_{\mathbf{t}}) = \lambda_{\mathbf{t}}, \partial H_{\mathbf{t}}/\partial(\delta\boldsymbol{u}_{\mathbf{t}}) = 0, \partial H_{\mathbf{t}}/\partial(\delta\boldsymbol{x}_N) = \lambda_N. \tag{13}$$

To improve the optimal control $\delta\boldsymbol{u}_{\mathbf{t}}$, the result costate equation is presented by solving (12)

$$\lambda_{\mathbf{k}} = \boldsymbol{A}_{\mathbf{t}}^T \delta\lambda_{\mathbf{t}+1} + Q(\delta\boldsymbol{x}_{\mathbf{t}} + \boldsymbol{x}_{\mathbf{t}}) \tag{14}$$

Based on the derivation of Hmiltonian with respect to $\delta u_{\mathbf{t}}$, the stationary condition is

$$R(\boldsymbol{u}_{\mathbf{t}} + \delta \boldsymbol{u}_{\mathbf{t}}) + \boldsymbol{B}_{\mathbf{t}}^{T} \delta \lambda_{\mathbf{t}+1} = 0 \tag{15}$$

The boundary condition is

$$\lambda_N = Q_f(\boldsymbol{x}_N + \delta \boldsymbol{x}_N - \boldsymbol{x}^*) \tag{16}$$

From the boundary equation (16), assuming

$$\lambda_{\mathbf{t}} = \mathbb{S}e_{\mathbf{t}} \delta \boldsymbol{x}_{\mathbf{t}} + \mathbb{V}_{\mathbf{t}} \tag{17}$$

Based on solving the equation (15) with (16) and substituting the result equation in (12) then combining this equation with (14), the optimal control error equation is presented as:

$$\delta \boldsymbol{u}_{\mathbf{t}} = -K \delta \boldsymbol{x}_{\mathbf{t}} - K_v \mathbb{V}_{\mathbf{t}+1} - K_u \boldsymbol{u}_{\mathbf{t}}. \tag{18}$$

The thrust and torque control error equations of the system are considered in the following :

$$\delta F_{\mathbf{t}} = -K \delta \xi_{\mathbf{t}} - K_v \mathbb{V}_{\mathbf{t}+1} - K_F F_{\mathbf{t}} \tag{19}$$

$$\delta M_{\mathbf{t}} = -K \delta \Omega_{\mathbf{t}} - K_v \mathbb{V}_{\mathbf{t}+1} - K_M M_{\mathbf{t}} \tag{20}$$

Consequently,

$$K = (\boldsymbol{B}_{\mathbf{t}}^T \mathbb{S}_{\mathbf{t}+1} \boldsymbol{B}_{\mathbf{t}} + R)^{-1} \boldsymbol{B}_{\mathbf{t}}^T \mathbb{S}_{\mathbf{t}+1} \boldsymbol{A}_{\mathbf{t}} \tag{21}$$

$$K_v = (\boldsymbol{B}_{\mathbf{t}}^T \mathbb{S}_{\mathbf{t}+1} \boldsymbol{B}_{\mathbf{t}} + R)^{-1} \boldsymbol{B}_{\mathbf{t}}^T \tag{22}$$

$$K_u = (\boldsymbol{B}_{\mathbf{t}}^T \mathbb{S}_{\mathbf{t}+1} \boldsymbol{B}_{\mathbf{t}} + R)^{-1} R. \tag{23}$$

The backward recursion equations $\mathbb{S}_{\mathbf{t}}$ and $\mathbb{V}_{\mathbf{t}}$ are used to solve the entire sequences of each iteration:

$$\mathbb{S}_{\mathbf{t}} = \boldsymbol{A}_{\mathbf{t}}^T \mathbb{S}_{\mathbf{t}+1} (\boldsymbol{A}_{\mathbf{t}} - B_{\mathbf{t}} K) + Q \tag{24}$$

$$\mathbb{V}_{\mathbf{t}} = (\boldsymbol{A}_{\mathbf{t}} - \boldsymbol{B}_{\mathbf{t}} K)^T \mathbb{V}_{\mathbf{t}+1} - K^T R \boldsymbol{u}_{\mathbf{t}} + Q \boldsymbol{x}_{\mathbf{t}} \tag{25}$$

where the gains K and K_u depend on the Riccati equation while the gain K_v is relevant on auxiliary sequence (25).

The improved control sequences $F_{\mathbf{t}}^*$ and $M_{\mathbf{t}}^*$ are originated from summation of the nominal control and the three terms of control derivation relying on thrust and torque van den Berg (2014) shown as:

$$F_{\mathbf{t}}^* = F_{\mathbf{t}} + \delta F_{\mathbf{t}} \tag{26}$$
$$M_{\mathbf{t}}^* = M_{\mathbf{t}} + \delta M_{\mathbf{t}}. \tag{27}$$

4. SIMULATION RESULTS

The iLQR optimal controller is tested for a slung load by cables with two quadrotors for the transportation task to track a desired spiral trajectory using MATLAB simulator. The applied parameters for this simulation are shown in table I.

Symbol	Definition	Value	Units
$\boldsymbol{I}_{Qx}^k$	Roll Inertia	4.4×10^-3	$kg.m^2$
$\boldsymbol{I}_{Qy}^k$	Pitch Inertia	4.4×10^-3	$kg.m^2$
$\boldsymbol{I}_{Qz}^k$	Yaw Inertia	8.8×10^-3	$kg.m^2$
m_Q^1	Mass	0.55	kg
m_Q^2	Mass	0.55	kg
m_P	Mass	0.2	kg
g	Gravity	9.81	m/s^2
L_Q^k	Arm Length	0.17	m
L_r^k	Rope Length	1	m
I_r	Rotor Inertia	4.4×10^-5	$kg.m^2$

Table 2. Quadrotor parameters

A spiral path is considered to control the load position attitudes, and quadrotors attitudes according to the equilibrium assumptions using the iLQR controller. The equilibrium point for the system is $\alpha^1 = 90$, $\alpha^2 = 90$, $\beta^1 = 45$ and $\beta^2 = -45$. The angle range limits are $\alpha^1 \in (0, 180)$, $\alpha^2 \in (0, 180)$, $\beta^1 \in (-90, 90)$ and $\beta^2 \in (-90, 90)$. The desired path tracked by the suspended load is presented by $x_d = 0.2tsin(0.3t), y_d = 0.2tcos(0.3t)$ and $z_d = 1 + t/10$. The iLQR simulation results are illustrated in figures then compared with the LQR controller results, where the sampling time is 0.001 sec and the running time is 40 sec. Furthermore, the weight matrices Q , R and Qf for the system are chosen to be positive parameters in diagonal matrices to determine the desired thrust and orientations.

$$Q = diag([1000, 100, 1000, 100, 1000, 100, 100, 0, 100, 0, 1000, 0, 1000, 0, 1000, 0, 100, 0, 100, 0, 1000, 0, 1000, 0, 1000, 0])$$

$$Qf = diag([1000, 10, 1000, 10, 1000, 10, 100, 0, 100, 0, 1000, 0, 1000, 0, 1000, 10, 100, 0, 100, 0, 1000, 0, 1000, 0, 10, 0])$$

$$R = diag([0.0001, 0.001, 0.0001, 0.001, 0.0001, 0.001, 0.0001, 0.001])$$

The performance of transporting the cable suspended payload with two quadrotors are illustrated in Figures 2-7. The payload position in Figure 2 shows a more stable performance and converges more quickly to the desired trajectory using the iLQR controller than the LQR controller. The first and second quadrotor attitude are shown in Figure 3 and Figure 4. Although all the Euler angles are not very close to the desired ones, the yaw angles from both quadrotors by the iLQR controller are more stable than the LQR controller. The payload angles with respect to the first and second quadrotor are shown in Figures 5 and 6, respectively. Again these angles controlled by the iLQR controller outperform the ones by iLQR controller as they have less oscillations.

The 3D animation trajectory using the iLQR controller is shown in Figure 7. It clearly shows the payload is able to track the desired trajectory. To compare the iLQR and LQR controller, the 3D trajectories are projected onto 2D space in Figures 8 and 9. The trajectory controlled by the iLQR controller is better than that by the LQR controller.

In summary, the iLQR controller performance is stable, faster and produces smaller steady state error than the LQR controller. But it requires more computational time due to the iteration.

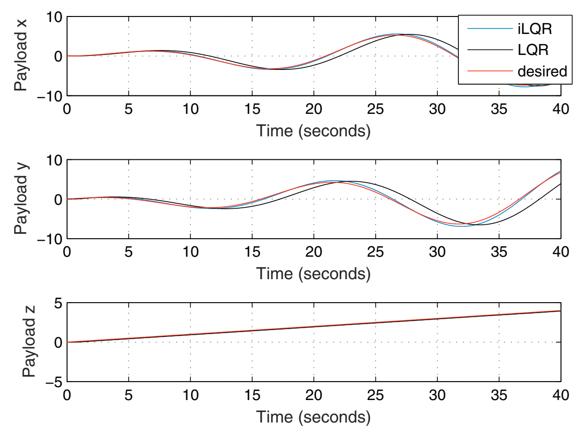

Fig. 2. Payload position representation for LQR and iLQR controllers

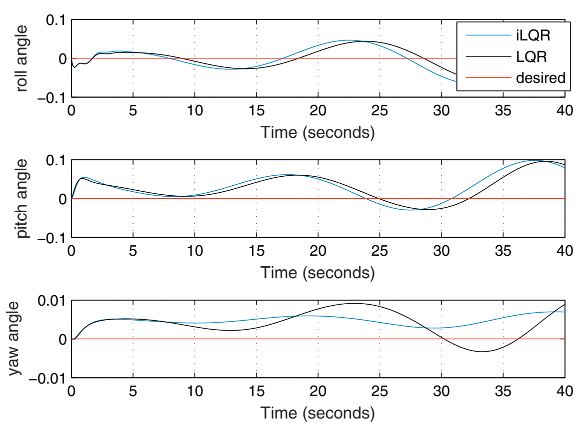

Fig. 3. The first quadrotor angles for spiral trajectory using IQR and iLQR controllers

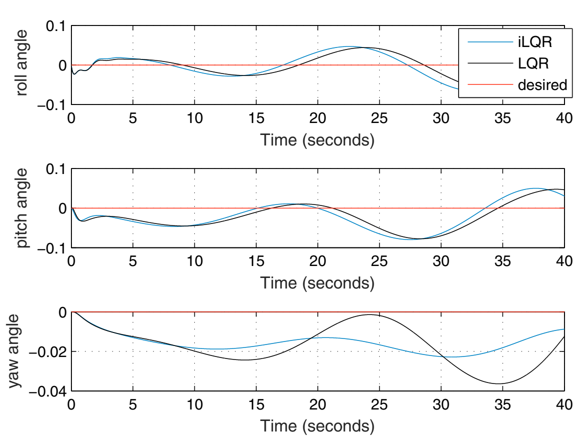

Fig. 4. The second quadrotor angles for spiral trajectory using LQR and iLQR Controllers

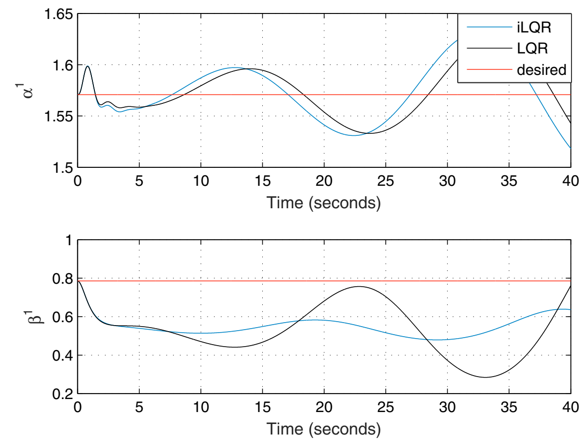

Fig. 5. Angels of the first quadrotor-load rope for spiral trajectory using LQR and iLQR Controllers

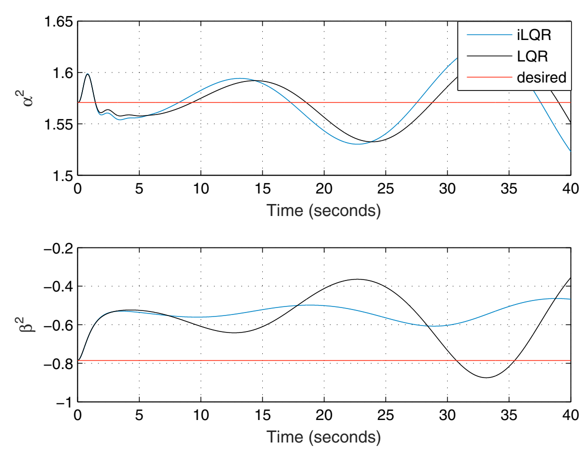

Fig. 6. Angels of the second quadrotor-load rope for spiral trajectory using LQR and iLQR Controllers

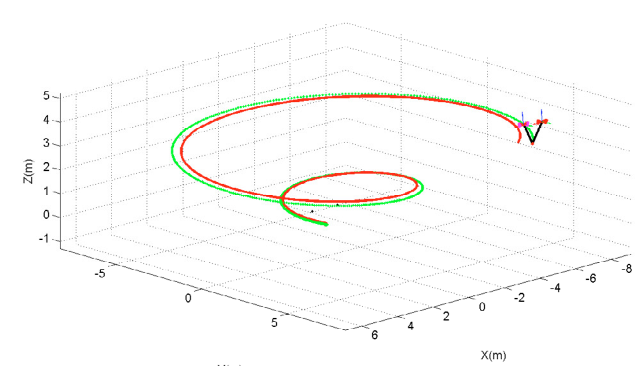

Fig. 7. 3D load position using iLQR Controller

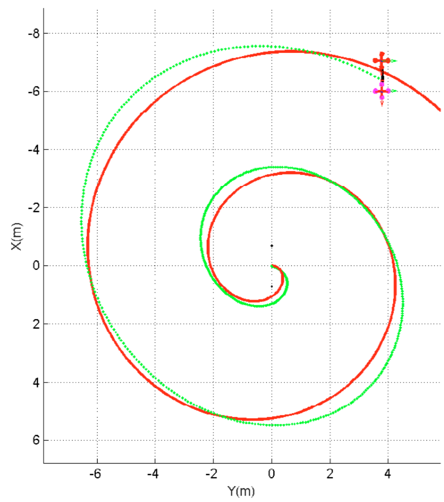

Fig. 8. 2D load position using LQR Controller

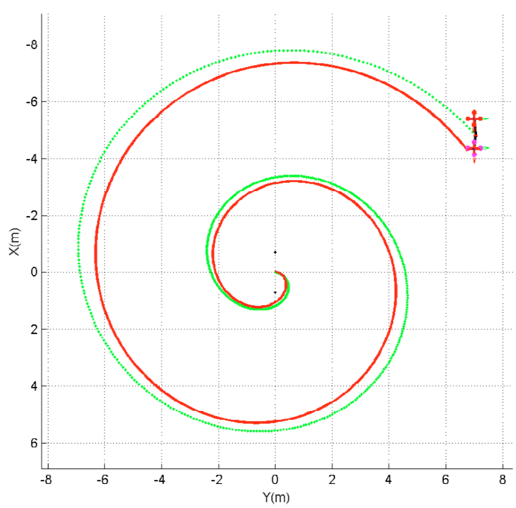

Fig. 9. 2D load position using iLQR Controller

5. CONCLUSION

In this paper, the iLQR optimal controller is developed for one cable suspended load with two quadrotors to achieve the transportation task along with a desired trajectory. The proposed controller was implemented and tested in simulation compared with a LQR controller. The results show that the iLQR controller is stable and outperforms the LQR controller. This indicates the iteration of iLQR is able to compensate for the load impact on the underlying system dynamics and the changes in operating point induced by the slung load. The next step work is to implement the iLQR controller for suspended load with two quadrotors by cables in real experiments.

REFERENCES

Alothman, Y., Jasim, W., and Gu, D. (2015). Quadrotor lifting-transporting cable-suspended payloads control. In *Automation and Computing (ICAC), 2015 21st International Conference on*, 1–6. IEEE.

de Crousaz, C., Farshidian, F., and Buchli, J. (2014). Aggressive optimal control for agile flight with a slung load. In *IEEE/RSJ International Conference on Intelligent Robots and Systems (IROS) Workshop on Machine Learning in Planning and Control of Robot Motion*.

de Crousaz, C., Farshidian, F., Neunert, M., and Buchli, J. (2015). Unified motion control for dynamic quadrotor maneuvers demonstrated on slung load and rotor failure tasks. In *Robotics and Automation (ICRA), 2015 IEEE International Conference on*, 2223–2229. IEEE.

Ghamry, K.A. and Zhang, Y. (2015). Formation control of multiple quadrotors based on leader-follower method. In *Unmanned Aircraft Systems (ICUAS), 2015 International Conference on*, 1037–1042. IEEE.

Klausen, K., Fossen, T.I., and Johansen, T.A. (2015). Nonlinear control of a multirotor UAV with suspended load. In *Unmanned Aircraft Systems (ICUAS), 2015 International Conference on*, 176–184. IEEE.

Lee, B.Y., Hong, S.M., Yoo, D.W., Lee, H.I., Moon, G.H., and Tahk, M.J. (2015). Design of a neural network controller for a slung-load system lifted by 1 quad-rotor. *Journal of Automation and Control Engineering Vol*, 3(1).

Lee, T. (2014). Geometric control of multiple quadrotor uavs transporting a cable-suspended rigid body. In *53rd IEEE Conference on Decision and Control*, 6155–6160. IEEE.

Lee, T., Sreenath, K., and Kumar, V. (2013). Geometric control of cooperating multiple quadrotor UAVs with a suspended payload. In *52nd IEEE Conference on Decision and Control*, 5510–5515. IEEE.

Li, W. and Todorov, E. (2004). Iterative linear quadratic regulator design for nonlinear biological movement systems. In *ICINCO (1)*, 222–229.

Sreenath, K. and Kumar, V. (2013). Dynamics, control and planning for cooperative manipulation of payloads suspended by cables from multiple quadrotor robots. *rn*, 1(r2), r3.

Trachte, J.E., Gonzalez Toro, L.F., and McFadyen, A. (2015). Multi-rotor with suspended load: System dynamics and control toolbox. In *Aerospace Conference, 2015 IEEE*, 1–9. IEEE.

van den Berg, J. (2014). Iterated LQR smoothing for locally-optimal feedback control of systems with nonlinear dynamics and non-quadratic cost. In *American Control Conference (ACC), 2014*, 1912–1918. IEEE.

Wu, G. and Sreenath, K. (2014). Geometric control of multiple quadrotors transporting a rigid-body load. In *53rd IEEE Conference on Decision and Control*, 6141–6148. IEEE.

Zhang, H.j., Gong, J.w., Jiang, Y., Xiong, G.m., and Chen, H.y. (2012). An iterative linear quadratic regulator based trajectory tracking controller for wheeled mobile robot. *Journal of Zhejiang University SCIENCE C*, 13(8), 593–600.